Iterative Maximum Likelihood Detection for Initial Ranging Process in 802.16 OFDMA Systems

Qiwei Wang and Guangliang Ren, *Member, IEEE*

***Abstract*—An iterative maximum likelihood detection (IMLD) algorithm is proposed for the contention based orthogonal frequency-division multiple access (OFDMA) initial ranging (IR) process compliant with the IEEE 802.16 specifications. In contrast to the existing successive interference cancellation (SIC) based algorithms, which suffer both the impacts of channel estimation errors as well as uncanceled multiple access interference (MAI), the proposed IMLD cancels the reconstructed MAI from the received signal by iteratively constructing an objective function derived from the EM algorithm. This approach could implement the maximum likelihood detection in an adaptive way with the MAI decreasing over iterations. Theoretical analyses and Cramër-Rao lower bounds (CRLBs) to the accuracy of parameters estimation are also provided. Simulation results show that the IMLD is of quick convergence, and significantly improves the performance of multiuser detection and parameters estimation with lower complexity compared to available algorithms.**

***Index Terms*—Orthogonal frequency division multiple access, initial ranging process, multiuser detection and estimation, iterative maximum likelihood detection.**

I. Introduction

A CONTENTION based initial ranging (IR) process is specified in orthogonal frequency-division multiple access (OFDMA) based 802.16 standards [1], by which signals of subscriber stations (SSs) arriving at the base station (BS) can be aligned to local timing and frequency references to avoid inter-carrier interference (ICI) and multiple access interference (MAI). In the IR process, the BS is required to detect code-divided multiuser ranging signals that spread over the same ranging channel, and extract their corresponding timing offsets as well as power levels for further data transmission. With the rapid development of the Internet-of-things (IOT), a large number of SSs, not only user terminals but also radio nodes, are necessary to establish uplink synchronization [2], indicating that it is a challenging task to improve the capacity and detection performance of the IR process.

To effectively detect multiuser ranging signals and estimate their corresponding parameters, by exploiting the orthogonality of ranging codes, several conventional single user detection (SUD) algorithms [3]–[6] are proposed to distinguish different ranging signals colliding in the same ranging channel. As ranging signals from different ranging subscriber stations (RSSs) suffer both the frequency selectivity of wireless channels and the phase shift which results because of timing offsets, the orthogonality among ranging codes is greatly damaged, giving rise to serious MAI. As a result, the performance of these algorithms degrades drastically.

One possible solution to combat the MAI is proposed in [7]–[10]. The basic idea is to assign special ranging sub-channels to different RSSs by dividing the wideband ranging channel into narrowband sub-channels, each of which could be regarded as a flat fading channel and can support a few RSSs. However, the reduction in the number of subcarriers degrades the timing estimation performance, offsetting the advantages of these schemes. Furthermore, these schemes cannot be applied into commercial systems based on the IEEE 802.16 standard.

Another possible solution to mitigate the MAI is the successive interference cancellation (SIC) based algorithms [11]–[13], the key challenging issues of which are the estimation of detected signals and interference cancellation based on it. One SIC based algorithm is proposed in [11] by exploiting the successive multi-user detection (SMUD), which takes the advantage of multipath channels by deeming the received ranging signal as many replicas of different active codes. From strong to weak, all active channel paths are detected and cancelled from the received signal over iterations, while in each iteration only the parameters of the strongest path should be estimated. With the increase in the number of iterations, the MAI is suppressed and weak channel paths are possible to be detected. The other SIC based algorithm is proposed in [12] and [13] by exploiting the criterion of generalized likelihood ratio test (GLRT) to detect possible ranging codes. Instead of estimating parameters of channel paths, the GLRT estimates the channel impulse response (CIR) of each detected code by using the maximum likelihood estimation (MLE) derived for one single code, and the SIC processing is implemented by canceling the reconstructed signals. However, the SIC based algorithms [11]–[13] suffer a problem that the SIC processing should be directly operated onto the received signal. At the initial stage of the SIC processing, the detection of certain channel path or code is impacted by strong MAI, resulting in inaccurate channel estimation. The channel estimation errors would be accumulated into the received signal after each SIC processing and cannot be mitigated anymore, along with uncanceled MAI (due to the rest of undetected channel paths or codes), impairing

Manuscript received December 17, 2013; revised May 9, 2014 and October 14, 2014; accepted January 7, 2015. Date of publication January 19, 2015; date of current version May 7, 2015. This work was supported by the National Natural Science Foundation of China (61072102), the National Key Science and Technology Projects of China (2011ZX03001-007-01), and the National Key Basic Research Program of China (973 Program, 2014CB340205). The associate editor coordinating the review of this paper and approving it for publication was A. Vosoughi.

The authors are with State Key Laboratory of ISN, Xidian University, Xi'an 710071, China (e-mail: merling870113@163.com).

Digital Object Identifier 10.1109/TWC.2015.2393308

the performance of these algorithms, especially when there are a large amount of RSSs. In addition, as three parameters need to be pre-designed by simulation results, the GLRT is not a constant false-alarm-rate (CFAR) detector, and cannot support as many RSSs as the SMUD. Therefore, in what follows, only the SMUD algorithm is taken into consideration for a comparison.

To mitigate the problem of existing algorithms, an iterative maximum likelihood detection (IMLD) algorithm is proposed in this work. The IMLD is derived from the classical EM algorithm [14], which has been widely used for the design of code division multiple access (CDMA) [15]–[17] and multi-carriers CDMA (MC-CDMA) receivers [18], [19]. However, unlike those common CDMA/MC-CDMA receivers, the IR detectors are demanded to detect the activities and estimate the parameters of ranging codes with the impact of strong MAI, rather than to extract the information each code carries. Several challenges are also faced, e.g., the number of active RSSs and their corresponding ranging codes are blind to the BS, no pilots are designated for channel estimation, and a large scope of timing offsets exist due to unsynchronized RSSs. To deal with these challenges, the IMLD is derived in the framework of the EM algorithm. In the expectation step (E-step), the conditional log-likelihood function is presented for each possible active channel path and an objective function is then derived. After that, the maximization step (M-step) is utilized to achieve the MLE of the current channel path. As the number of active channel paths is blind to the BS, the IMLD is designed into an adaptive form to check the validity of each possible channel path and accommodate different detection results over iterations. Compared with existing IR detectors, the proposed IMLD is able to provide better detection performance and larger IR capacity. Furthermore, as the general Cramër-Rao lower bounds (CRLBs) for multiuser parameters estimation in the IR have not been provided before, they are also derived.

This paper is arranged as follows. Section II describes the signal model of the IR process briefly. Section III derives the IMLD in the framework of the EM algorithm, and presents its implementation with some issues in detail discussed. In Section IV, theoretical analyses about the IMLD and CRLBs to the accuracy of parameters estimation are derived. Simulation parameters and numerical results are shown in Section V, and the conclusion is presented in Section VI.

The following notations are used in this paper. Matrices and vectors are denoted by boldface letters, and $\mathbf{0}$ represents an all-zero matrix. $\mathbf{A} = diag\{a(n), n = 0, 1, \ldots, N-1\}$ denotes an $N \times N$ diagonal matrix with entries $a(n)$ along its main diagonal. The notations $E(\cdot)$, $(\cdot)^T$, $(\cdot)^H$ are utilized for expectation, transposition and Hermitian transposition.

II. Signal Model

The system model is on the basis of IEEE 802.16 family standards [1], and an OFDMA system with $\mathcal{M}$ subcarriers is considered. The ranging opportunity is consist of M subcarriers with indices $\{\mathcal{J}_m, 0 \leqslant m \leqslant M-1\}$ in two OFDMA symbols, where m is the index of ranging subcarriers and code elements. After downlink synchronization, each RSS should send a ranging code to notify the request of network entry, which is randomly selected from a code set that contains several binary phase-shift keying (BPSK) ranging codes. Defining the number of ranging codes by N, the code set is denoted as $\mathbb{C} = [\mathbf{C}_1, \ldots, \mathbf{C}_{\mathfrak{N}}, \ldots, \mathbf{C}_N]$, and the $\mathfrak{N}^{\text{th}}$ code is given as

$$\mathbf{C}_{\mathfrak{N}} = [C_{\mathfrak{N}}(0), \ldots, C_{\mathfrak{N}}(m), \ldots, C_{\mathfrak{N}}(M-1)]^T, \tag{1}$$

where $C_{\mathfrak{N}}(m)$ is the m^{th} element of the $\mathfrak{N}^{\text{th}}$ ranging code.

Assuming the code $\mathbf{C}_{\mathfrak{N}_k}$ is randomly selected by the k^{th} RSS, where $1 \leqslant \mathfrak{N}_k \leqslant N$, the code is fed to an inverse discrete Fourier transform (IDFT) to form the time domain signal as

$$S_k(n) = \frac{1}{\sqrt{\mathcal{M}}} \sum_{m=0}^{M-1} C_{\mathfrak{N}_k}(m) e^{j2\pi \frac{\mathcal{J}_m}{\mathcal{M}} n}. \tag{2}$$

The resulting signal is extended over two OFDMA symbols by being repeated twice with prefix and suffix added. Without loss of generality, one assumes the ranging slot is shared by V data subscriber stations (DSSs) and K RSSs. The signals of RSSs and DSSs respectively propagate through the multi-path channels and arrive at the BS with corresponding round-trip delays (RTDs). The received signal is expressed as

$$y(n) = \sum_{k=1}^{K} \sum_{l=0}^{L-1} h_k[l] \cdot S_k(n-l-d_k) + \sum_{v=1}^{V} \sum_{l=0}^{L-1} h_v[l] \cdot X_v(n-l) + w(n), \tag{3}$$

where $h_k[l]$ is the coefficient of the l^{th} channel path of the k^{th} RSS, $h_v[l]$ is the coefficient of the l^{th} channel path of the v^{th} DSS, $L-1$ is the maximum channel delay spread, d_k is the RTD of the k^{th} RSS, $X_v(n)$ denotes the time domain signal of the v^{th} DSS, and $w(n)$ accounts for additive white Gaussian noise (AWGN) samples with zero-mean and variance of σ_w^2. The RTDs of DSSs are not taken into consideration due to the established uplink synchronization.

As the first OFDMA symbol actually acts as a prolonged prefix for the second one, only the second OFDMA symbol is utilized for further processing. The samples of the second OFDMA symbol are transferred into the frequency domain by using a discrete Fourier transform (DFT). In what follows, the impact of DSS signals on RSS signals is neglected as they are frequency-divided. The received overlapped ranging signal is then extracted from the ranging channel as

$$Y(\mathcal{J}_m) = \sum_{k=1}^{K} \sum_{l=0}^{L-1} h_k[l] \Phi_m(\tau_k[l]) C_{\mathfrak{N}_k}(m) + W(\mathcal{J}_m), \tag{4}$$

where $\tau_k[l] \triangleq d_k + l$ is defined as the timing offset of the l^{th} channel path of the k^{th} RSS, $\Phi_m(\tau_k[l]) = e^{-j2\pi \frac{\mathcal{J}_m}{\mathcal{M}} \tau_k[l]}$ denotes the phase shift which results because of the timing offset, and $W(\mathcal{J}_m)$ is the AWGN in the frequency domain.

The received signal could be represented in matrix forms as

$$\mathbf{Y} = \sum_{k=1}^{K} \sum_{l=0}^{L-1} h_k[l] \mathbf{\Gamma}(\tau_k[l]) \mathbf{C}_{\mathfrak{N}_k} + \mathbf{W}, \tag{5}$$

where

$$\mathbf{Y} = [Y(\mathcal{J}_0), \ldots, Y(\mathcal{J}_m), \ldots, Y(\mathcal{J}_{M-1})]^T \quad (6)$$

$$\mathbf{W} = [W(\mathcal{J}_0), \ldots, W(\mathcal{J}_m), \ldots, W(\mathcal{J}_{M-1})]^T \quad (7)$$

$$\mathbf{\Gamma}(\tau_k[l]) = diag\{\Phi_m(\tau_k[l]), 0 \leqslant m \leqslant M-1\}. \quad (8)$$

In what follows, the possible collision when several RSSs choose the same ranging code is neglected since a scheduled transmission following by the multiuser detection procedure is regulated by the BS to check possible collisions and notify the collided RSSs to initiate a new IR process [1].

III. Iterative Maximum Likelihood Detection

In this section, the ranging signal model is re-expressed for the convenience of further analyses. The objective function of the IMLD according to the EM algorithm is derived, and the implementation along with some detail issues are depicted.

A. Re-Expression of System Model

As the BS is required to detect and estimate active channel paths among all possible ones, the received signal could be re-expressed as a linear combination of all active channel paths that are blind to the BS.

Let the maximum RTD be $d_{\max}$, the number of all possible timing offsets is defined as $\tau_{\max} = d_{\max} + L$, and the set of possible timing offsets $\mathbb{T} \triangleq [0, \tau_{\max} - 1]$. As the number of ranging codes is N, there are total $N \times \tau_{\max}$ possible channel paths. Among all the possible channel paths, we assume there are $\mathfrak{L}_{\mathfrak{N}}$ active ones for the $\mathfrak{N}^{\text{th}}$ code with $\mathfrak{L}_{\mathfrak{N}} \leqslant L$. The received signal in (5) is re-expressed in terms of all ranging codes and their corresponding active channel paths as

$$\mathbf{Y} = \sum_{\mathfrak{N}=1}^{N} \sum_{\ell=1}^{\mathfrak{L}_{\mathfrak{N}}} h_{\mathfrak{N},\ell} \mathbf{\Gamma}(\tau_{\mathfrak{N},\ell}) \mathbf{C}_{\mathfrak{N}} + \mathbf{W}, \quad (9)$$

where ℓ is the index of active channel paths for each code, $h_{\mathfrak{N},\ell}$ and $\tau_{\mathfrak{N},\ell}$ are the channel coefficient and timing offset of the ℓ^{th} active channel path of the $\mathfrak{N}^{\text{th}}$ code. For a given ranging code, if none of its channel paths is valid, this code is inactive, i.e., $\mathfrak{L}_{\mathfrak{N}} = 0$; on the other hand, if any of its channel paths is valid, this code is supposed to be active, i.e., $\mathfrak{L}_{\mathfrak{N}} > 0$.

B. Construction of Objective Function

Define $\Psi_{\mathfrak{N},\ell} = [h_{\mathfrak{N},\ell}, \tau_{\mathfrak{N},\ell}] \in \Theta$ as the parameter vector of the ℓ^{th} active channel path of the $\mathfrak{N}^{\text{th}}$ code with its estimation represented as $\widehat{\Psi}_{\mathfrak{N},\ell} = [\widehat{h}_{\mathfrak{N},\ell}, \widehat{\tau}_{\mathfrak{N},\ell}] \in \widehat{\Theta}$, where Θ denotes the set of parameter vectors of all the active channel paths and $\widehat{\Theta}$ contains the latest estimation results of all the channel paths.

By utilized the re-expressed signal model and definitions above, according to the terminology of the EM algorithm, the received signal could be regarded as the so-called incomplete data (observed data), and the signal of each active channel path could be deemed as the complete data. The expectation step (E-step) and maximization step (M-step) of the IMLD could be given as follows.

E-Step:

$$Q\left(\Psi_{\mathfrak{N},\ell} \middle| \widehat{\Theta}\right) \triangleq \ln \mathcal{P}\left(\mathbf{Y} \middle| \Psi_{\mathfrak{N},\ell}, \widehat{\Theta}\right) \propto -\left\|(\mathbf{Y} - \widehat{\boldsymbol{\kappa}}_{\mathfrak{N},\ell}) - h_{\mathfrak{N},\ell}\mathbf{\Gamma}(\tau_{\mathfrak{N},\ell})\mathbf{C}_{\mathfrak{N}}\right\|^2, \quad (10)$$

where

$$\widehat{\boldsymbol{\kappa}}_{\mathfrak{N},\ell} \triangleq \sum_{\mathfrak{M}=1}^{N} \sum_{\Upsilon=1}^{\mathfrak{L}_{\mathfrak{M}}} \widehat{h}_{\mathfrak{M},\Upsilon} \mathbf{\Gamma}(\widehat{\tau}_{\mathfrak{M},\Upsilon}) \mathbf{C}_{\mathfrak{M}} - \widehat{h}_{\mathfrak{N},\ell} \mathbf{\Gamma}(\widehat{\tau}_{\mathfrak{N},\ell}) \mathbf{C}_{\mathfrak{N}}. \quad (11)$$

M-Step:

$$\widehat{\Psi}_{\mathfrak{N},\ell} = \arg\max \left\{ Q\left(\Psi_{\mathfrak{N},\ell} \middle| \widehat{\Theta}\right) \right\}. \quad (12)$$

The validity of the current possible path is then checked by using the estimation results in (12), and the valid estimated parameter vector is updated into the set of estimation results as $\widehat{\Psi}_{\mathfrak{N},\ell} \to \widehat{\Theta}$. The IMLD is proceeded between the E-step and M-step until a pre-designed terminating condition is satisfied.

To derive the MLE of (12), calculating the derivative of (10) with respect to $h_{\mathfrak{N},\ell}$ by keeping $\tau_{\mathfrak{N},\ell}$ fixed and letting the derivative equal zero yield

$$\widehat{h}_{\mathfrak{N},\ell} = \frac{1}{M} \mathbf{C}_{\mathfrak{N}}^H \mathbf{\Gamma}^H(\tau_{\mathfrak{N},\ell})(\mathbf{Y} - \widehat{\boldsymbol{\kappa}}_{\mathfrak{N},\ell}). \quad (13)$$

Bringing (13) back into (10) while calculating the derivative with respect to $\tau_{\mathfrak{N},\ell}$ and letting it equal zero produce

$$\widehat{\tau}_{\mathfrak{N},\ell} = \arg\max_{\tau \in \mathbb{T}} \left| \mathbf{C}_{\mathfrak{N}}^H \mathbf{\Gamma}^H(\tau)(\mathbf{Y} - \widehat{\boldsymbol{\kappa}}_{\mathfrak{N},\ell}) \right|. \quad (14)$$

Thus the channel estimate of the current path is given by

$$\widehat{h}_{\mathfrak{N},\ell} = \frac{1}{M} \mathbf{C}_{\mathfrak{N}}^H \mathbf{\Gamma}^H(\widehat{\tau}_{\mathfrak{N},\ell})(\mathbf{Y} - \widehat{\boldsymbol{\kappa}}_{\mathfrak{N},\ell}). \quad (15)$$

According to (14) and (15), we define $\mathbf{T}_{\mathfrak{N},\ell} = \mathbf{Y} - \widehat{\boldsymbol{\kappa}}_{\mathfrak{N},\ell}$ as the objective function for the detection of the current possible channel path. In what follows, the objective function is utilized to form the E-step of the IMLD and the derived results in (14) and (15) are used as the M-step of the IMLD.

C. Practical Implementation

From the descriptions above, it is known that the IMLD is implemented by detecting all active channel paths with the objective function constructed according to the EM algorithm. However, as the active channel paths are blind to the BS, the IMLD must be designed into an adaptive way to accommodate the uncertainty of the number of active channel paths. Some issues in detail also need to be dealt with, e.g., the initialization, determination of the validity of each possible path, terminating conditions, and so on. In what follows, the practical implementation of the IMLD is introduced in detail and a diagram of the IMLD is depicted in Fig. 1.

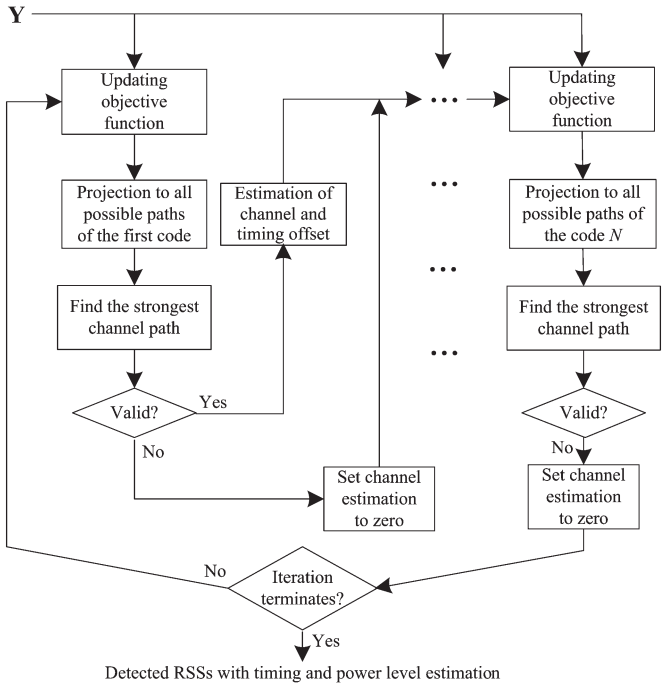

Fig. 1. An illustrative diagram of the IMLD.

1) Initialization: The matrices of estimates of channel coefficients and timing offsets are defined as

$$\mathbf{h}^{(i)} = \left[\mathbf{h}_1^{(i)}, \ldots, \mathbf{h}_{\mathfrak{N}}^{(i)}, \ldots, \mathbf{h}_N^{(i)}\right]^T \tag{16}$$

$$\boldsymbol{\tau}^{(i)} = \left[\boldsymbol{\tau}_1^{(i)}, \ldots, \boldsymbol{\tau}_{\mathfrak{N}}^{(i)}, \ldots, \boldsymbol{\tau}_N^{(i)}\right]^T, \tag{17}$$

where

$$\mathbf{h}_{\mathfrak{N}}^{(i)} = \left[\widehat{h}_{\mathfrak{N},1}^{(i)}, \ldots, \widehat{h}_{\mathfrak{N},\ell}^{(i)}, \ldots, \widehat{h}_{\mathfrak{N},\mathfrak{L}_{\mathfrak{N}}[i]}^{(i)}\right] \tag{18}$$

$$\boldsymbol{\tau}_{\mathfrak{N}}^{(i)} = \left[\widehat{\tau}_{\mathfrak{N},1}^{(i)}, \ldots, \widehat{\tau}_{\mathfrak{N},\ell}^{(i)}, \ldots, \widehat{\tau}_{\mathfrak{N},\mathfrak{L}_{\mathfrak{N}}[i]}^{(i)}\right]. \tag{19}$$

Note that $\mathfrak{L}_{\mathfrak{N}}[i]$ is the number of active channel paths that are detected by the IMLD in the i^{th} iteration. The iteration is initialized by setting $i = 0$, $\mathfrak{L}_{\mathfrak{N}}[0] = 0$, $\boldsymbol{\tau}^{(0)} = \mathbf{0}$ and $\mathbf{h}^{(0)} = \mathbf{0}$. Since $\mathfrak{L}_{\mathfrak{N}}[i]$ is based on the estimated results in each iteration, if false or duplicate detections of certain channel paths happen, it is possible that $\mathfrak{L}_{\mathfrak{N}}[i] > \mathfrak{L}_{\mathfrak{N}}$; otherwise, $\mathfrak{L}_{\mathfrak{N}}[i] \leqslant \mathfrak{L}_{\mathfrak{N}}$ as some active but weak channel paths may not be detected.

2) Processing in Each Iteration: In each iteration, the IMLD is proceeded in an order from one code to another to detect all possible active paths. In the i^{th} iteration, taking into account the possible channel path $\Psi_{\mathfrak{N},\ell}$ as the current one to be re-detected and re-estimated, its objective function is constructed as (20), shown at the bottom of the page. It is obviously seen that the reconstructed MAI is consist of two parts. One is the reconstructed MAI obtained by using the updated estimation results in the current iteration, and the other is the reconstructed MAI obtained according to the estimation results in the previous iteration.

The two-dimensional grid-search correlation processing in (14) and (15) with normalized power is then defined as

$$Corr_{\mathfrak{N},\ell}^{(i)}(\tau) \triangleq \mathbf{C}_{\mathfrak{N}}^H \boldsymbol{\Gamma}^H(\tau) \mathbf{T}_{\mathfrak{N},\ell}^{(i)} \Big/ \sqrt{\left(\mathbf{T}_{\mathfrak{N},\ell}^{(i)}\right)^H \mathbf{T}_{\mathfrak{N},\ell}^{(i)}}, \tag{21}$$

where $\tau \in \mathbb{T}$ is the index of all possible timing offsets.

The current path should be determined active or not by using all the correlation values from (21). If $\max|Corr_{\mathfrak{N},\ell}^{(i)}(\tau)| \geqslant \eta$, where η is a pre-designed threshold, the timing offset and channel coefficient of the current path are re-estimated as

$$\widehat{\tau}_{\mathfrak{N},\ell}^{(i)} = \arg\max_{\tau \in \mathbb{T}} \left| Corr_{\mathfrak{N},\ell}^{(i)}(\tau) \right| \tag{22}$$

$$\widehat{h}_{\mathfrak{N},\ell}^{(i)} = \frac{1}{M} Corr_{\mathfrak{N},\ell}^{(i)}\left(\widehat{\tau}_{\mathfrak{N},\ell}^{(i)}\right) \sqrt{\left(\mathbf{T}_{\mathfrak{N},\ell}^{(i)}\right)^H \mathbf{T}_{\mathfrak{N},\ell}^{(i)}}. \tag{23}$$

And the detection for the next possible channel path of the current code should continue being implemented. Otherwise, if $\max|Corr_{\mathfrak{N},\ell}^{(i)}(\tau)| < \eta$, the current channel path is unlikely to be valid. In this case, the detection for the current code is terminated with $\mathfrak{L}_{\mathfrak{N}}[i] = \ell - 1$, and the next code should then be proceeded. After the detection of all possible ranging codes is completed in each iteration, it should be decided whether the IMLD terminates or not as follows.

3) Terminating Conditions: The IMLD terminates when the maximum number of iterations $\gamma_{\max}$ is reached. Besides, to alleviate the complexity, the IMLD could terminate ahead of schedule by defining an early terminating threshold λ. After each iteration, the root mean-square error (RMSE) of channel estimates between two successive iterations is given as

$$RMSE_h^{(i)} = \frac{\sqrt{\left\|\mathbf{h}^{(i)} - \mathbf{h}^{(i-1)}\right\|^2}}{\sum_{\mathfrak{N}=1}^{N} \left[\max\left\{\mathfrak{L}_{\mathfrak{N}}[i-1], \mathfrak{L}_{\mathfrak{N}}[i]\right\}\right]}. \tag{24}$$

Note the dimensions of $\mathbf{h}^{(i)}$ and $\mathbf{h}^{(i-1)}$ should be adjusted the same by zero padding. If $RMSE_h^{(i)} < \lambda$, the IMLD terminates prematurely; otherwise, the next iteration shall restart back to step 2) unless the maximum number of iterations is reached.

$$\mathbf{T}_{\mathfrak{N},\ell}^{(i)} = \mathbf{Y} - \underbrace{\left[\sum_{\mathfrak{M}=1}^{\mathfrak{N}-1} \sum_{\Upsilon=1}^{\mathfrak{L}_{\mathfrak{M}}[i]} \widehat{h}_{\mathfrak{M},\Upsilon}^{(i)} \boldsymbol{\Gamma}\left(\widehat{\tau}_{\mathfrak{M},\Upsilon}^{(i)}\right) \mathbf{C}_{\mathfrak{M}} + \sum_{\Upsilon=1}^{\ell-1} \widehat{h}_{\mathfrak{N},\Upsilon}^{(i)} \boldsymbol{\Gamma}\left(\widehat{\tau}_{\mathfrak{N},\Upsilon}^{(i)}\right) \mathbf{C}_{\mathfrak{N}}\right]}_{\text{Reconstructed MAI via the estimation results in the current iteration}}$$
$$- \underbrace{\left[\sum_{\Upsilon=\ell+1}^{\mathfrak{L}_{\mathfrak{N}}[i-1]} \widehat{h}_{\mathfrak{N},\Upsilon}^{(i-1)} \boldsymbol{\Gamma}\left(\widehat{\tau}_{\mathfrak{N},\Upsilon}^{(i-1)}\right) \mathbf{C}_{\mathfrak{N}} + \sum_{\mathfrak{M}=\mathfrak{N}+1}^{N} \sum_{\Upsilon=1}^{\mathfrak{L}_{\mathfrak{M}}[i-1]} \widehat{h}_{\mathfrak{M},\Upsilon}^{(i-1)} \boldsymbol{\Gamma}\left(\widehat{\tau}_{\mathfrak{M},\Upsilon}^{(i-1)}\right) \mathbf{C}_{\mathfrak{M}}\right]}_{\text{Reconstructed MAI via the estimation results in the privious iteration}} \tag{20}$$

4) Code Detection and Parameters Estimation: Once the IMLD terminates, we define the number of iterations it performs as γ_{IMLD}. For each ranging code, it should be checked whether active or not as

$$\begin{cases} \text{If } \mathfrak{L}_{\mathfrak{N}}[\gamma_{\text{IMLD}}] > 0, & \text{Code } \mathfrak{N} \text{ is active} \\ \text{If } \mathfrak{L}_{\mathfrak{N}}[\gamma_{\text{IMLD}}] = 0, & \text{Code } \mathfrak{N} \text{ is inactive} \end{cases} \tag{25}$$

As the matrices $\mathbf{h}^{(\gamma_{\text{IMLD}})}$ and $\boldsymbol{\tau}^{(\gamma_{\text{IMLD}})}$ contain the final estimation results of channel coefficients and timing offsets, the estimates of RTD and power level of each code are given as

$$\widehat{d}_{\mathfrak{N}} = \min_{\ell \in [1, \mathfrak{L}_{\mathfrak{N}}[\gamma_{\text{IMLD}}]]} \widehat{\tau}_{\mathfrak{N},\ell}^{(\gamma_{\text{IMLD}})} \tag{26}$$

$$\widehat{P}_{\mathfrak{N}} = \sum_{\ell=1}^{\mathfrak{L}_{\mathfrak{N}}[\gamma_{\text{IMLD}}]} \left| \widehat{h}_{\mathfrak{N},\ell}^{(\gamma_{\text{IMLD}})} \right|^2. \tag{27}$$

D. Remarks

1) As the IMLD needs to compute (21) when detecting each possible channel path, the method to simplify (21) has been proposed in [5], which shows the two dimensional grid-search correlation processing can be computed by one inverse fast Fourier transform (IFFT) for a given code with all possible timing offsets at a complexity of $O(\mathcal{M}\log_2\mathcal{M})$.
2) The path validation threshold is given as that in [11], i.e., $\eta = \sqrt{\log(\tau_{\max}) - \log(\mathcal{P}_{fa})}$, where $\mathcal{P}_{fa}$ is the desired false-alarm probability. It is derived by deeming the correlation values as complex Gaussian noises if a given code is inactive. Benefiting from the threshold, the IMLD is a CFAR detector as well, and the probability of a false detection could be limited low enough, facilitating the initialization as well.
3) Define the number of detections the IMLD requires as

$$L_P \triangleq \sum_{i=1}^{\gamma_{\text{IMLD}}} L_P[i] = \sum_{i=1}^{\gamma_{\text{IMLD}}} \sum_{\mathfrak{N}=1}^{N} \left(\mathfrak{L}_{\mathfrak{N}}[i] + 1\right), \tag{28}$$

where $L_P[i]$ is the number of detections in the i^{th} iteration. In each iteration, the IMLD needs to compute $L_P[i]$ operations of MLE, power normalization, signal reconstruction and subtraction, its total complexity is approximately $L_P(\mathcal{M}\log_2\mathcal{M} + 14\mathcal{M})$. While the SMUD requires N operations of MLE, and one operation of power normalization, signal reconstruction and subtraction in each iteration. If it has γ_{SMUD} iterations, its total complexity is $\gamma_{\text{SMUD}}(N\mathcal{M}\log_2\mathcal{M} + 14\mathcal{M})$. It is obviously seen that the complexity of both algorithms comes from the computation of IFFT operations, while the computational burden of other operations could be neglected. In this case, the numbers of IFFT operations are utilized to compare the complexities of both the algorithms in Section V.

IV. Performance Analyses

In this section, the mean square error (MSE) of channel estimation is derived, and the convergence and initialization of the IMLD are analyzed accordingly. The CRLBs to the accuracy of multiuser parameters estimation are also derived.

A. MSE of Channel Estimates, Convergence and Initialization

In this sub-section, we first analyze the MSE of channel estimates, based on which the convergence and initialization of the IMLD are discussed as well. According to (20), (21), and (23), the estimation of an active channel path $\Psi_{\mathfrak{N},\ell}$ is expressed as $\widehat{h}_{\mathfrak{N},\ell}^{(i)} = h_{\mathfrak{N},\ell} + \mathcal{A}_{\mathfrak{N},\ell}^{(i)}$, where $\mathcal{A}_{\mathfrak{N},\ell}^{(i)}$ represented in (29), shown at the bottom of the page, is the channel estimation error, $\varpi_{\mathfrak{N},\ell} \triangleq \frac{1}{M}\mathbf{C}_{\mathfrak{N}}^H\boldsymbol{\Gamma}^H(\tau_{\mathfrak{N},\ell})\mathbf{W}$ is defined as the cross-correlation of the current path with the AWGN, and $I_{\mathfrak{M},\Upsilon} \triangleq \frac{1}{M}\mathbf{C}_{\mathfrak{N}}^H\boldsymbol{\Gamma}^H(\tau_{\mathfrak{N},\ell}) \cdot \boldsymbol{\Gamma}(\tau_{\mathfrak{M},\Upsilon})\mathbf{C}_{\mathfrak{M}}$ is defined as one MAI item with $\mathfrak{N} \neq \mathfrak{M}$ or $\ell \neq \Upsilon$.

Note that $\varpi_{\mathfrak{N}\ell}$ is a linear combination of complex Gaussian noise samples with zero-mean and variance of σ_w^2/M. Following [11]–[13], the MAI items $I_{\mathfrak{M},\Upsilon}$ could be assumed as independent identical distributed (i.i.d.) complex Gaussian variables with zero-mean and variance of σ_S^2 ($\ll 1$), and the estimation errors could also be deemed as i.i.d. variables with zero-mean. Let us focus on the first iteration of the IMLD, the channel estimation error is expressed as (30), shown at the bottom of the page, and the MSE of the channel estimate is represented as

$$\begin{aligned} MSE\left[\widehat{h}_{\mathfrak{N},\ell}^{(1)}\right] &\triangleq E\left|\widehat{h}_{\mathfrak{N},\ell}^{(1)} - h_{\mathfrak{N},\ell}\right|^2 = E\left|\mathcal{A}_{\mathfrak{N},\ell}^{(1)}\right|^2 \\ &= \sigma_S^2\left[\sum_{\mathfrak{M}=1}^{\mathfrak{N}-1}\sum_{\Upsilon=1}^{\mathfrak{L}_{\mathfrak{M}}} E\left|\mathcal{A}_{\mathfrak{M},\Upsilon}^{(1)}\right|^2 + \sum_{\Upsilon=1}^{\ell-1} E\left|\mathcal{A}_{\mathfrak{N},\Upsilon}^{(1)}\right|^2 + \frac{\sigma_w^2}{M\sigma_S^2}\right. \\ &\qquad \left. + \sum_{\Upsilon=\ell+1}^{\mathfrak{L}_{\mathfrak{N}}} E\left|h_{\mathfrak{N},\Upsilon}\right|^2 + \sum_{\mathfrak{M}=\mathfrak{N}+1}^{N}\sum_{\Upsilon=1}^{\mathfrak{L}_{\mathfrak{M}}} E\left|h_{\mathfrak{M},\Upsilon}\right|^2\right]. \end{aligned} \tag{31}$$

$$\begin{aligned} \mathcal{A}_{\mathfrak{N},\ell}^{(i)} = \Bigg[&\sum_{\mathfrak{M}=1}^{\mathfrak{N}-1}\sum_{\Upsilon=1}^{\mathfrak{L}_{\mathfrak{M}}}\left(h_{\mathfrak{M},\Upsilon} - \widehat{h}_{\mathfrak{M},\Upsilon}^{(i)}\right)I_{\mathfrak{M},\Upsilon} + \sum_{\Upsilon=1}^{\ell-1}\left(h_{\mathfrak{N},\Upsilon} - \widehat{h}_{\mathfrak{N},\Upsilon}^{(i)}\right)I_{\mathfrak{N},\Upsilon} + \varpi_{\mathfrak{N},\ell} \\ &+ \sum_{\Upsilon=\ell+1}^{\mathfrak{L}_{\mathfrak{N}}}\left(h_{\mathfrak{N},\Upsilon} - \widehat{h}_{\mathfrak{N},\Upsilon}^{(i-1)}\right)I_{\mathfrak{N},\Upsilon} + \sum_{\mathfrak{M}=\mathfrak{N}+1}^{N}\sum_{\Upsilon=1}^{\mathfrak{L}_{\mathfrak{M}}}\left(h_{\mathfrak{M},\Upsilon} - \widehat{h}_{\mathfrak{M},\Upsilon}^{(i-1)}\right)I_{\mathfrak{M},\Upsilon}\Bigg] \end{aligned} \tag{29}$$

$$\mathcal{A}_{\mathfrak{N},\ell}^{(1)} = \left[-\sum_{\mathfrak{M}=1}^{\mathfrak{N}-1}\sum_{\Upsilon=1}^{\mathfrak{L}_{\mathfrak{M}}}\mathcal{A}_{\mathfrak{M},\Upsilon}^{(1)}I_{\mathfrak{M},\Upsilon} - \sum_{\Upsilon=1}^{\ell-1}\mathcal{A}_{\mathfrak{N},\Upsilon}^{(1)}I_{\mathfrak{N},\Upsilon} + \varpi_{\mathfrak{N},\ell} + \sum_{\Upsilon=\ell+1}^{\mathfrak{L}_{\mathfrak{N}}}h_{\mathfrak{N},\Upsilon}I_{\mathfrak{N},\Upsilon} + \sum_{\mathfrak{M}=\mathfrak{N}+1}^{N}\sum_{\Upsilon=1}^{\mathfrak{L}_{\mathfrak{M}}}h_{\mathfrak{M},\Upsilon}I_{\mathfrak{M},\Upsilon}\right] \tag{30}$$

As pointed in [11] that the IR detectors work well unless the MAI and AWGN are extremely large, if a certain channel path is detected, due to $\sigma_S^2 \ll 1$, it is reasonable to assume

$$E\left|\mathcal{A}_{\mathfrak{N},\ell}^{(1)}\right|^2 < E|h_{\mathfrak{N},\ell}|^2, \tag{32}$$

meaning that the MSE of channel estimation of one detected path should be statistically smaller than its expected power. After some easy algebras, a conclusion is obtained as

$$E\left|\mathcal{A}_{\mathfrak{N},\ell}^{(i+1)}\right|^2 < E\left|\mathcal{A}_{\mathfrak{N},\ell}^{(i)}\right|^2, \tag{33}$$

which indicates that the MSE of channel estimation of a detected channel path is decreasing over two successive iterations. This conclusion suggests that with the channel estimates of detected paths becoming more and more accurate, interference cancellation of the objective function becomes more effective, which further facilitates the detection of weak paths.

As the IMLD is proposed based on the EM algorithm, which has been proved convergent if proper initial values are selected [14], the conclusion also proves that the IMLD is convergent based on the assumption in (32), and the initialization issue of the IMLD is illustrated as follows. For one thing, the dispreading gain against MAI is supposed to be large enough, i.e., $\sigma_S^2 \ll 1$, which is in accordance with available CDMA/MC-CDMA receivers [15]–[19] or IR detectors [11]–[13] and benefits from the orthogonality of ranging codes. For another, the path validation threshold is able to refine the occurrence of false channel paths to the maximum extent, which guarantees the validity of the objective function. From this perspective, the initialization is actually its first iteration, benefiting from both the intrinsic dispreading gain of ranging codes, the path validation threshold, and the objective function.

B. CLRBs of Parameters Estimation

In available literature about the IR process, a theoretical analysis about multiuser parameters estimation has not been performed. To obtain the limiting performance, the CLRBs of estimates of timing offsets and power levels are derived. For the subsequent investigation, we define a new vector $\mathbf{\Omega}$ that contains the real and imaginary part of the channel coefficients as well as their corresponding timing offsets as

$$\begin{aligned}\mathbf{\Omega} &= [\Omega_1, \ldots, \Omega_b, \ldots, \Omega_{3\beta}] \\ &= \big[\Re(h_{1,1}), \ldots, \Re(h_{1,\mathfrak{L}_1}), \ldots, \Re(h_{\mathfrak{N},1}), \ldots, \Re\left(h_{\mathfrak{N},\mathfrak{L}_\mathfrak{N}}\right) \\ &\quad \Im(h_{1,1}), \ldots, \Im(h_{1,\mathfrak{L}_1}), \ldots, \Im(h_{\mathfrak{N},1}), \ldots, \Im\left(h_{\mathfrak{N},\mathfrak{L}_\mathfrak{N}}\right) \\ &\quad \tau_{1,1}, \ldots, \tau_{1,\mathfrak{L}_1}, \ldots, \tau_{\mathfrak{N},1}, \ldots, \tau_{\mathfrak{N},\mathfrak{L}_\mathfrak{N}}\big],\end{aligned} \tag{34}$$

where $\beta \triangleq \sum_{\mathfrak{N}=1}^{N} \mathfrak{L}_\mathfrak{N}$, $\Re$ and $\Im$ denote the real and imaginary part, respectively. The information inequality for the covariance matrix of any unbiased estimate follows

$$E\left[(\widehat{\mathbf{\Omega}} - \mathbf{\Omega})^T (\widehat{\mathbf{\Omega}} - \mathbf{\Omega})\right] \geqslant \mathbf{F}^{-1}(\mathbf{\Omega}), \tag{35}$$

where the $3\beta \times 3\beta$ positive definite real matrix $\mathbf{F}(\mathbf{\Omega})$ stands for the Fisher information matrix (FIM) of $\mathbf{\Omega}$. The mean-square estimation error (MSEE) is lower-bounded by

$$\begin{aligned}MSEE(\widehat{\Omega}_b) &\triangleq E\left[(\widehat{\Omega}_b - \Omega_b)^2\right] \\ &\geqslant \left[\mathbf{F}^{-1}(\mathbf{\Omega})\right]_{b,b} \triangleq CRLB(\Omega_b),\end{aligned} \tag{36}$$

where $[\cdot]_{b,b}$ is the element at the b^{th} row and column of a square matrix. The FIM is partitioned into 9 sub-matrices of dimension $\beta \times \beta$ as.

$$\mathbf{F}(\mathbf{\Omega}) = \begin{pmatrix} \mathbf{F}_{\Re\Re}(\mathbf{\Omega}) & \mathbf{F}_{\Re\Im}(\mathbf{\Omega}) & \mathbf{F}_{\Re\tau}(\mathbf{\Omega}) \\ \mathbf{F}_{\Re\Im}^T(\mathbf{\Omega}) & \mathbf{F}_{\Im\Im}(\mathbf{\Omega}) & \mathbf{F}_{\Im\tau}(\mathbf{\Omega}) \\ \mathbf{F}_{\Re\tau}^T(\mathbf{\Omega}) & \mathbf{F}_{\Im\tau}^T(\mathbf{\Omega}) & \mathbf{F}_{\tau\tau}(\mathbf{\Omega}) \end{pmatrix}. \tag{37}$$

The elements of the FIM defined above are expressed as $\mathbf{F}_{b,b'}(\mathbf{\Omega}) = -E[(\partial/\partial\Omega_b)(\partial/\partial\Omega_{b'})\ln(\mathcal{P}(\mathbf{Y}|\mathbf{\Omega}))]$, where $b, b' = 1, \ldots, 3\beta$. The second order derivative of the log-likelihood function is given in (38), shown at the bottom of the page. Defining $\alpha = \sum_{\mathfrak{M}=0}^{\mathfrak{N}-1} \mathfrak{L}_\mathfrak{M} + \ell$ and $\alpha' = \sum_{\mathfrak{M}=0}^{\mathfrak{N}'-1} \mathfrak{L}_\mathfrak{M} + \ell'$ with $\mathfrak{L}_0 = 0$, $1 \leq \mathfrak{N}, \mathfrak{N}' \leq N$, $1 \leq \ell \leq \mathfrak{L}_\mathfrak{N}$ and $1 \leq \ell' \leq \mathfrak{L}_{\mathfrak{N}'}$, the elements at the α^{th} row and $(\alpha')^{\text{th}}$ column of the partitioned sub-matrices are given as (39)–(43).

$$\begin{aligned}[\mathbf{F}_{\Re\Re}(\mathbf{\Omega})]_{\alpha,\alpha'} &= [\mathbf{F}_{\Im\Im}(\mathbf{\Omega})]_{\alpha,\alpha'} \\ &= \sum_{m=0}^{M-1} \frac{2}{\sigma_w^2} C_\mathfrak{N}(m) C_{\mathfrak{N}'}(m) \\ &\quad \times \begin{bmatrix} \Re\left(\Phi_m(\tau_{\mathfrak{N},\ell})\right) \Re\left(\Phi_m(\tau_{\mathfrak{N}',\ell'})\right) \\ +\Im\left(\Phi_m(\tau_{\mathfrak{N},\ell})\right) \Im\left(\Phi_m(\tau_{\mathfrak{N}',\ell'})\right) \end{bmatrix}\end{aligned} \tag{39}$$

$$\begin{aligned}[\mathbf{F}_{\Re\Im}(\mathbf{\Omega})]_{\alpha,\alpha'} &= \sum_{m=0}^{M-1} \frac{2}{\sigma_w^2} C_\mathfrak{N}(m) C_{\mathfrak{N}'}(m) \\ &\quad \times \begin{bmatrix} \Im\left(\Phi_m(\tau_{\mathfrak{N},\ell})\right) \Re\left(\Phi_m(\tau_{\mathfrak{N}',\ell'})\right) \\ -\Re\left(\Phi_m(\tau_{\mathfrak{N},\ell})\right) \Im\left(\Phi_m(\tau_{\mathfrak{N}',\ell'})\right) \end{bmatrix}\end{aligned} \tag{40}$$

$$\begin{aligned}[\mathbf{F}_{\Re\tau}(\mathbf{\Omega})]_{\alpha,\alpha'} &= \sum_{m=0}^{M-1} \frac{4\pi \mathcal{J}_m}{M\sigma_w^2} C_\mathfrak{N}(m) C_{\mathfrak{N}'}(m) \\ &\quad \times \Re\left(\Phi_m(\tau_{\mathfrak{N},\ell})\right) \begin{bmatrix} \Im(h_{\mathfrak{N}',\ell'}) \Re\left(\Phi_m(\tau_{\mathfrak{N}',\ell'})\right) \\ +\Re(h_{\mathfrak{N}',\ell'}) \Im\left(\Phi_m(\tau_{\mathfrak{N}',\ell'})\right) \end{bmatrix} \\ &\quad + \sum_{m=0}^{M-1} \frac{4\pi \mathcal{J}_m}{M\sigma_w^2} C_\mathfrak{N}(m) C_{\mathfrak{N}'}(m) \\ &\quad \times \Im\left(\Phi_m(\tau_{\mathfrak{N},\ell})\right) \begin{bmatrix} \Im(h_{\mathfrak{N}',\ell'}) \Im\left(\Phi_m(\tau_{\mathfrak{N}',\ell'})\right) \\ -\Re(h_{\mathfrak{N}',\ell'}) \Re\left(\Phi_m(\tau_{\mathfrak{N}',\ell'})\right) \end{bmatrix}\end{aligned} \tag{41}$$

$$\begin{aligned}-\frac{\partial}{\partial\Omega_b}\frac{\partial}{\partial\Omega_b'}\ln(\mathcal{P}(\mathbf{Y}|\mathbf{\Omega})) &= \frac{1}{\sigma_w^2}\frac{\partial}{\partial\Omega_b}\frac{\partial}{\partial\Omega_b'}\left\{\sum_{m=0}^{M-1}\left|Y(\mathcal{J}_m) - \sum_{\mathfrak{N}=1}^{N}\sum_{\ell=1}^{\mathfrak{L}_\mathfrak{N}} h_{\mathfrak{N},\ell}\cdot\Phi_m(\tau_{\mathfrak{N},\ell})C_\mathfrak{N}(m)\right|^2\right\} \\ &= \frac{1}{\sigma_w^2}\frac{\partial}{\partial\Omega_b}\frac{\partial}{\partial\Omega_b'}\sum_{m=0}^{M-1}\left\{\begin{array}{l}\left[\Re\left(Y(\mathcal{J}_m)\right) - \sum_{\mathfrak{N}=1}^{N}\sum_{\ell=1}^{\mathfrak{L}_\mathfrak{N}} C_\mathfrak{N}(m)\left(\Re(h_{\mathfrak{N},\ell})\Re\left(\Phi_m(\tau_{\mathfrak{N},\ell})\right) - \Im(h_{\mathfrak{N},\ell})\Im\left(\Phi_m(\tau_{\mathfrak{N},\ell})\right)\right)\right]^2 \\ +\left[\Im\left(Y(\mathcal{J}_m)\right) - \sum_{\mathfrak{N}=1}^{N}\sum_{\ell=1}^{\mathfrak{L}_\mathfrak{N}} C_\mathfrak{N}(m)\left(\Re(h_{\mathfrak{N},\ell})\Im\left(\Phi_m(\tau_{\mathfrak{N},\ell})\right) + \Im(h_{\mathfrak{N},\ell})\Re\left(\Phi_m(\tau_{\mathfrak{N},\ell})\right)\right)\right]^2\end{array}\right\}\end{aligned} \tag{38}$$

$$[\mathbf{F}_{\Im\tau}(\mathbf{\Omega})]_{\alpha,\alpha'} = -\sum_{m=0}^{M-1}\frac{4\pi\jmath_m}{M\sigma_w^2}C_{\mathfrak{N}}(m)C_{\mathfrak{N}'}(m) \times \Im\left(\Phi_m(\tau_{\mathfrak{N},\ell})\right)\begin{bmatrix}\Re(h_{\mathfrak{N}',\ell'})\Im\left(\Phi_m(\tau_{\mathfrak{N}',\ell'})\right)\\ +\Im(h_{\mathfrak{N}',\ell'})\Re\left(\Phi_m(\tau_{\mathfrak{N}',\ell'})\right)\end{bmatrix} + \sum_{m=0}^{M-1}\frac{4\pi\jmath_m}{M\sigma_w^2}C_{\mathfrak{N}}(m)C_{\mathfrak{N}'}(m) \times \Re\left(\Phi_m(\tau_{\mathfrak{N},\ell})\right)\begin{bmatrix}\Im(h_{\mathfrak{N}',\ell'})\Im\left(\Phi_m(\tau_{\mathfrak{N}',\ell'})\right)\\ -\Re(h_{\mathfrak{N}',\ell'})\Re\left(\Phi_m(\tau_{\mathfrak{N}',\ell'})\right)\end{bmatrix} \quad (42)$$

$$[\mathbf{F}_{\tau\tau}(\mathbf{\Omega})]_{\alpha,\alpha'} = \sum_{m=0}^{M-1}\frac{8\pi^2\jmath_m^2}{M^2\sigma_w^2}C_{\mathfrak{N}}(m)C_{\mathfrak{N}'}(m) \times\begin{bmatrix}\Re(h_{\mathfrak{N},\ell})\Im\left(\Phi_m(\tau_{\mathfrak{N},\ell})\right)\\ +\Im(h_{\mathfrak{N},\ell})\Re\left(\Phi_m(\tau_{\mathfrak{N},\ell})\right)\end{bmatrix}\begin{bmatrix}\Im(h_{\mathfrak{N}',\ell'})\Re\left(\Phi_m(\tau_{\mathfrak{N}',\ell'})\right)\\ +\Re(h_{\mathfrak{N}',\ell'})\Im\left(\Phi_m(\tau_{\mathfrak{N}',\ell'})\right)\end{bmatrix} + \sum_{m=0}^{M-1}\frac{8\pi^2\jmath_m^2}{M^2\sigma_w^2}C_{\mathfrak{N}}(m)C_{\mathfrak{N}'}(m) \times\begin{bmatrix}\Re(h_{\mathfrak{N},\ell})\Re\left(\Phi_m(\tau_{\mathfrak{N},\ell})\right)\\ -\Im(h_{\mathfrak{N},\ell})\Im\left(\Phi_m(\tau_{\mathfrak{N},\ell})\right)\end{bmatrix}\begin{bmatrix}\Re(h_{\mathfrak{N}',\ell'})\Re\left(\Phi_m(\tau_{\mathfrak{N}',\ell'})\right)\\ -\Im(h_{\mathfrak{N}',\ell'})\Im\left(\Phi_m(\tau_{\mathfrak{N}',\ell'})\right)\end{bmatrix} \quad (43)$$

Generally, one can assume that channel coefficients follow i.i.d. complex Gaussian distribution with zero-mean, and that timing offsets follow i.i.d. uniform distribution. The CRLBs could be loosened by integrating the FIM over the distribution of $\mathbf{\Omega}$. Therefore, the sub-matrices $\mathbf{F}_{\Re\Im}(\mathbf{\Omega})$, $\mathbf{F}_{\Re\tau}(\mathbf{\Omega})$ and $\mathbf{F}_{\Im\tau}(\mathbf{\Omega})$ become zero matrices, and the elements of $\mathbf{F}_{\Re\Re}(\mathbf{\Omega})$ and $\mathbf{F}_{\Im\Im}(\mathbf{\Omega})$ are expressed as

$$[\mathbf{F}_{\Re\Re}(\mathbf{\Omega})]_{\alpha,\alpha'} = [\mathbf{F}_{\Im\Im}(\mathbf{\Omega})]_{\alpha,\alpha'} = \begin{cases}\frac{2}{\sigma_w^2}M, & \alpha=\alpha'\\ \frac{2}{\sigma_w^2}\sum_{m=0}^{M-1}C_{\mathfrak{N}}(m)C_{\mathfrak{N}'}(m)\frac{2[1-cos(\vartheta_m(\tau_{\max}-1))]}{\vartheta_m^2\tau_{\max}^2}, & \alpha\neq\alpha'\end{cases} \quad (44)$$

where $\vartheta_m = -2\pi\frac{\jmath_m}{M}$. According to the standard [1], due to the existence of guard bands and virtual subcarriers, we have $0 \ll \frac{\jmath_m}{M} < 1$. As $\tau_{\max}$ is a pretty large value, we have $\frac{2[1-cos(\vartheta_m(\tau_{\max}-1))]}{\vartheta_m^2\tau_{\max}^2} \to 0$. Further, by combining with the orthogonality among different ranging codes, $\mathbf{F}_{\Re\Re}(\mathbf{\Omega})$ and $\mathbf{F}_{\Im\Im}(\mathbf{\Omega})$ could be approximately deemed as diagonal matrices.

Also, the sub-matrix $\mathbf{F}_{\tau\tau}(\mathbf{\Omega})$ is a diagonal matrix with diagonal elements given as

$$[\mathbf{F}_{\tau\tau}(\mathbf{\Omega})]_{\alpha,\alpha} = \frac{8\pi^2|h_{\mathfrak{N},\ell}|^2\sum_{m=0}^{M-1}\jmath_m^2}{M^2\sigma_w^2}. \quad (45)$$

The discussion above indicates the CRLB can be computed once the knowledge about the noise variance and PDP of the wireless channel is available. The diagonal elements of $\mathbf{F}^{-1}(\mathbf{\Omega})$ are approximately the reciprocals of that of $\mathbf{F}(\mathbf{\Omega})$ as

$$CRLB\left(\Re(h_{\mathfrak{N},\ell})\right) = CRLB\left(\Im(h_{\mathfrak{N},\ell})\right) = \left[\mathbf{F}_{\Re\Re}^{-1}(\mathbf{\Omega})\right]_{\alpha,\alpha} = \left[\mathbf{F}_{\Im\Im}^{-1}(\mathbf{\Omega})\right]_{\alpha,\alpha} \approx \frac{\sigma_w^2}{2M} \quad (46)$$

$$CRLB(\tau_{\mathfrak{N},\ell}) = \left[\mathbf{F}_{\tau\tau}^{-1}(\mathbf{\Omega})\right]_{\alpha,\alpha} \approx \frac{M^2\sigma_w^2}{8\pi^2|h_{\mathfrak{N},\ell}|^2\sum_{m=0}^{M-1}\jmath_m^2} \quad (47)$$

As the RTD is exactly the delay of the first channel path, the CRLB to the accuracy of RTD estimation is given as

$$CRLB(d_{\mathfrak{N}}) = CRLB(\tau_{\mathfrak{N},1}) \approx \frac{M^2\sigma_w^2}{8\pi^2|h_{\mathfrak{N},1}|^2\sum_{m=0}^{M-1}\jmath_m^2} \quad (48)$$

Recalling that $P_{\mathfrak{N}} = \sum_{\ell=1}^{\mathfrak{L}_{\mathfrak{N}}}|h_{\mathfrak{N},\ell}|^2 = \sum_{\ell=1}^{\mathfrak{L}_{\mathfrak{N}}}[\Re(h_{\mathfrak{N},\ell})^2+\Im(h_{\mathfrak{N},\ell})^2]$, the CRLB to the accuracy of power estimation is given as [20]

$$\begin{aligned}CRLB(P_{\mathfrak{N}}) &\approx \sum_{\ell=1}^{\mathfrak{L}_{\mathfrak{N}}}\left[\frac{\partial P_{\mathfrak{N}}}{\partial\Re(h_{\mathfrak{N},\ell})}\right]^2 CRLB\left(\Re(h_{\mathfrak{N},\ell})\right) + \sum_{\ell=1}^{\mathfrak{L}_{\mathfrak{N}}}\left[\frac{\partial P_{\mathfrak{N}}}{\partial\Im(h_{\mathfrak{N},\ell})}\right]^2 CRLB\left(\Im(h_{\mathfrak{N},\ell})\right)\\ &= \frac{2\sigma_w^2}{M}\sum_{\ell=1}^{\mathfrak{L}_{\mathfrak{N}}}|h_{\mathfrak{N},\ell}|^2. \end{aligned} \quad (49)$$

V. Simulation Results

A. Simulation Parameters

The simulation parameters are chosen in compliance with the IEEE 802.16m standard specified in [1]. The FFT size is 1024 with a CP composed of 128 samples, and the sampling frequency is 11.2 MHz, corresponding to a subcarrier spacing of 11.16 kHz. The system bandwidth is 10 MHz and the carrier frequency is 2.3 GHz. A cell radius of 1 km is considered, indicating that the maximum RTD corresponding to a RSS on the cell border is 114 samples. There are 80 subcarriers on both sides as guard bands, and the residual 864 subcarriers are used for the IR and data transmission. These subcarriers are grouped into tiles, each containing 4 adjacent subcarriers. A sub-channel is consisting of 6 non-consecutive tiles. The total ranging subcarriers are composed by 6 sub-channels, meaning that there are 144 ranging subcarriers. The number of ranging codes allocated for the IR is 40. The carrier frequency offset (CFO) is less than 2% of the subcarrier spacing. The probability of false-alarm (FA) is kept within 1×10^{-3} and the channel model is set to be the ITU-R M.1225 Vehicle-A channel with the mobile speed of 60 km/h.

B. Simulation Results

1) Selection of Maximum Number of Iterations: Fig. 2 shows the miss-detection probability with respect to the maximum number of iterations. The number of RSSs is selected as 6 or 10 under the SNR of 0 dB or 20 dB, and the early terminating threshold is not utilized here. It is seen that when the maximum number of iterations exceeds 6, the detection performance keeps constant in all these cases, indicating that the IMLD achieves the best detection performance at the 6th iteration and no further improvement could be brought by spending more iterations. As a result, the maximum number of iterations is selected as 6 in what follows.

2) Selection of Early Terminating Threshold: Figs. 3 and 4 show the miss-detection probability and number of iterations with respect to the early terminating threshold λ, where "Lambda" stands for λ. It is seen that the detection performance

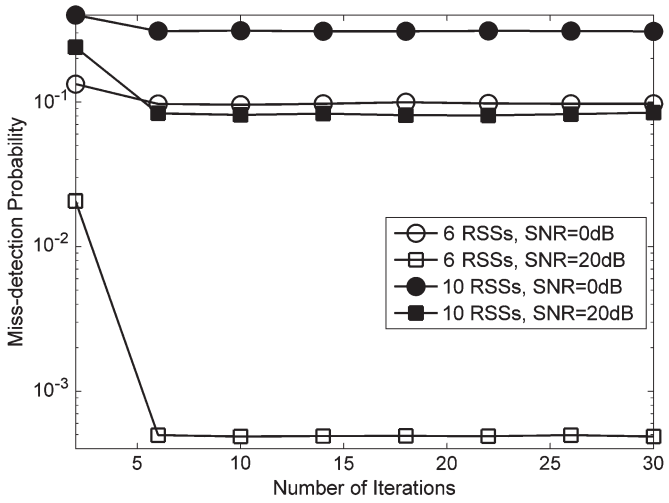

Fig. 2. Miss-detection performance vs. different numbers of iterations.

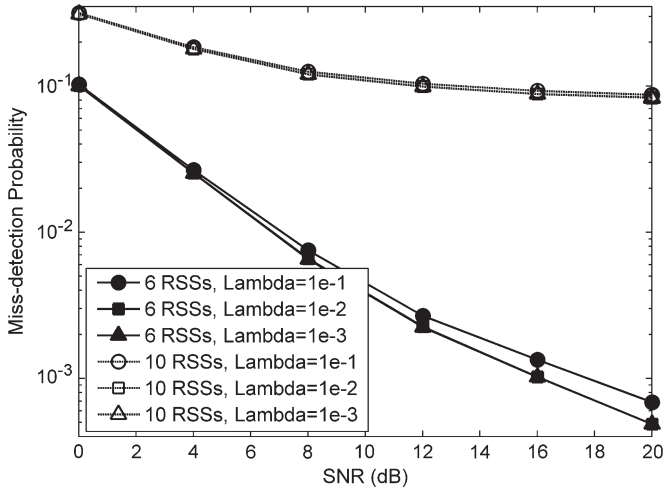

Fig. 3. Miss-detection performance vs. different values of Lambda.

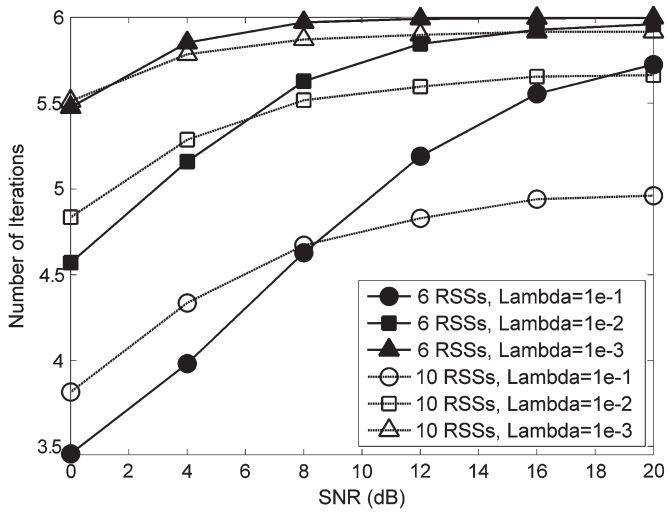

Fig. 4. Number of iterations vs. different values of Lambda.

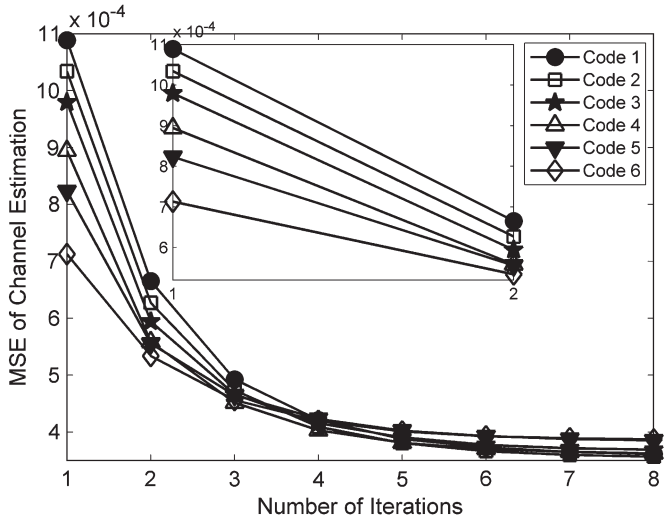

Fig. 5. MSE of channel estimation.

is slightly improved with λ decreasing from 1×10^{-1} to 1×10^{-2}. However, with λ decreasing from 1×10^{-2} to 1×10^{-3}, there is no further improvement in the detection performance but more iterations are cost. This indicates that 1×10^{-2} is supposed to be small enough to be an indicator for the IMLD to terminate prematurely, which could achieve an optimal performance while lowering the complexity to the maximum extent.

3) MSE of Channel Estimation: Fig. 5 shows the MSE of channel estimation with respect to the number of iterations when the SNR is 10 dB, providing a test to verify the convergence of the IMLD. The detection order is on the basis of the index of ranging codes. It is shown that with the increase in the number of iterations, the MSE of channel estimation decreases. In the first iteration, since "code 1" is the first one to be estimated, large MAI exists such that the MSE of "code 1" is the largest among all active codes. With the objective function constructed in the first iteration, the MSE of channel estimation decreases with the increase in the index of codes. In the second iteration, the MSE of channel estimation of the same code decreases drastically compared to that in the first iteration, indicating that the simulation result is compliant with the conclusion in (33) and that the IMLD is covergent. Furthermore, the MSE of channel estimation of different codes become stabilized at the 6th iteration, which further verifies that the selection of maximum number of iterations as 6 is large enough for the IMLD to converge.

4) Comparison of Detection and Estimation Performances: Fig. 6 shows the comparison of miss-detection performance between the IMLD and the SMUD. On one hand, the detection performance of the IMLD outperforms that of the SMUD significantly. When the SNR is 0 dB, the miss-detection probabilities decrease from 1.14×10^{-1}, 2.06×10^{-1}, 3.53×10^{-1} to 9.80×10^{-2}, 1.78×10^{-1}, 3.08×10^{-1} with the number of active RSSs being 6, 8, and 10, respectively. When the SNR is 20 dB, the miss-detection probabilities decrease from 3.50×10^{-3}, 3.52×10^{-2}, 1.35×10^{-1}, to 5.02×10^{-4}, 1.31×10^{-2}, 8.22×10^{-2} with the number of active RSSs being 6, 8, and 10, respectively. This indicates that the performance enhancement becomes more and more significant with the increase in the SNR. On the other hand, the detection performance of both algorithms degrades with the increase in the number of RSSs, suggesting that the MAI is the dominant factor impairing the multiuser detection and estimation performance.

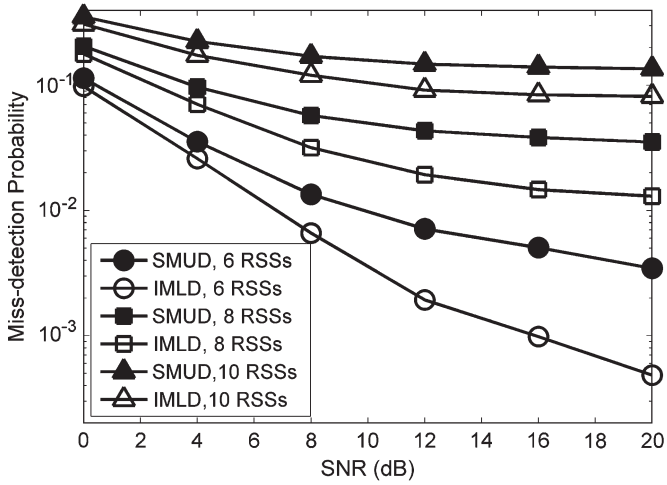

Fig. 6. Comparison of miss-detection performance.

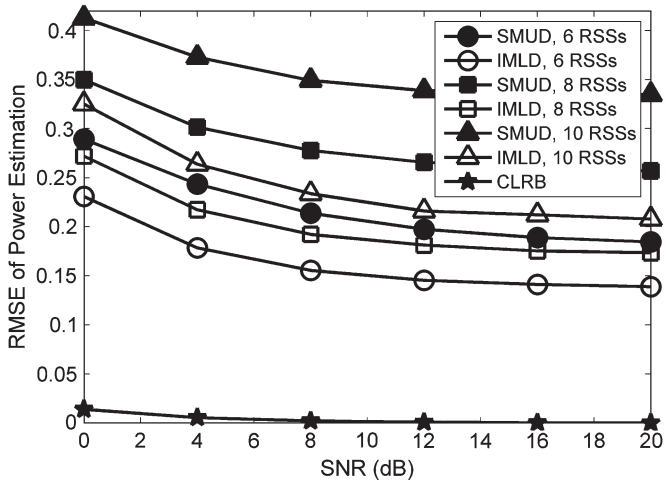

Fig. 8. Comparison of normalized RMSE of power level estimation.

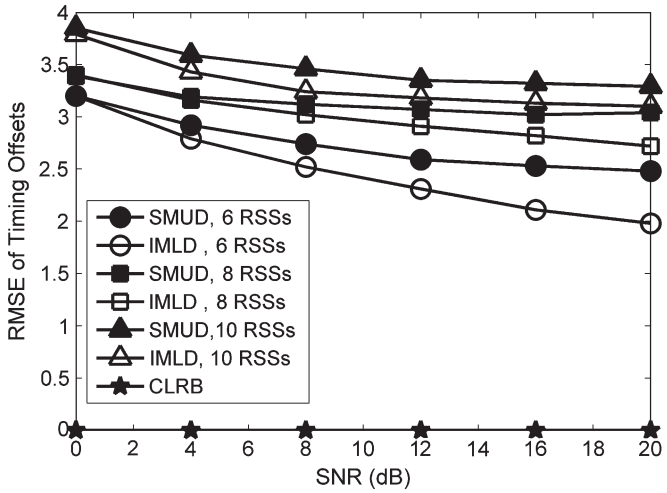

Fig. 7. Comparison of RMSE of timing offset estimation.

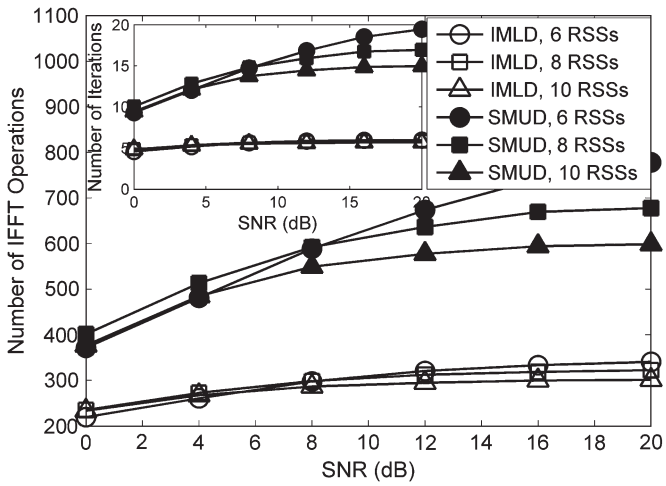

Fig. 9. Comparison of complexity.

The CRLBs to the accuracy of mutliuser parameters estimation are also presented by using the simulation parameters given above, which are in accordance with the assumptions in Section IV-B, i.e., the channel coefficients and timing offsets are i.i.d. variables, and the PDP of the wireless channel is known. Therefore, the CRLBs are calculated according to (48), (49) and are presented in Fig. 7 and Fig. 8.

Fig. 7 shows the comparison of timing offsets estimation between the IMLD and the SMUD. It can be seen that the CLRB of timing offsets estimation approaches zeros under different SNR conditions, while the RMSEs of timing offsets estimation of both algorithms are at least 2 samples larger than the CLRB. When the SNR is 0 dB, both algorithms have almost the same performance of timing offsets estimation. With the increase in the SNR, the timing offsets estimation of the IMLD grows more accurate than that of the SMUD.

Fig. 8 shows the comparison of power estimation between the IMLD and the SMUD. The CRLB of power estimation is less than 0.027 when the SNR exceeds 0 dB while the RMSEs of power estimation of both algorithms are larger than 0.1. As the power estimate depends on the estimation of possible channel paths, the result shows that the accuracy of power estimation of the IMLD greatly outperforms that of the SMUD, further verifying that the IMLD could provide more accurate channel estimation and better MAI mitigation than the SMUD.

5) Comparison of Complexities: Fig. 9 shows the comparison of complexity between the IMLD and the SMUD. It can be obviously seen that the number of IFFT operations the IMLD requires is much smaller than that of the SMUD. When the SNR is 0 dB, the IMLD only requires 200 to 240 IFFT operations, while the SMUD approximately 370 to 400 ones. With the increase in the SNR, both algorithms necessitate more complexities since more weak channel paths could be detected. When the SNR is 20 dB, the IMLD requires 300 to 350 IFFT operations, while the SMUD 600 to 750 ones. Furthermore, it is noticed that in the SMUD, the number of IFFT operations is proportional to the number of iterations since it requires N times IFFT operations in each iteration. While in the IMLD, the number of IFFT operations is approximately proportional to the number of iterations as the average number of detected channel paths per iteration is fixed in a statistical sense. Therefore, combining with the simulation results shown in Figs. 6–9, we can come to a conclusion that the IMLD is able to achieve better multiuser detection and estimation performance with relatively lower complexity than the SMUD.

VI. Conclusion

Aiming at improving the detection performance and capacity of the IR process, the IMLD is proposed in the framework of the classical EM algorithm. Through the derivations of the E-step and M-step for the IMLD, an objective function is constructed to perform the MLE for each active channel path in an adaptive way while mitigating the MAI for each path over iterations. The implementation of the IMLD is illustrated with several issues in detail discussed. Theoretical analyses about the channel estimation, convergence, and initialization of the IMLD are performed, and CRLBs to the accuracy of multiuser parameters estimation are presented since the limiting performance for the IR process has not been provided before. With a considerable decrease in the complexity, the IMLD is able to achieve better detection performance than existing algorithms. In addition, it is worth noting that once the MAI and AWGN are extremely large, although not employed in this paper, an ordered IMLD could be further adopted by re-arranging the code indexes from strong to weak according the power estimation results of the SUD at the initialization stage and that of the IMLD after each iteration.

References

[1] *IEEE Standard for Local and Metropolitan Area Networks, Part 16: Air Interface for Broadband Wireless Access Systems Amendment 3: Advanced Air Interface*, IEEE 802.16m, May 2011.

[2] A. Laya, L. Alonso, and J. Alonso-Zarate, "Is the random access channel of LTE and LTE-A suitable for M2M communications? A survey of alternatives," *IEEE Commun. Surveys Tuts.*, vol. 16, no. 1, pp. 4–16, Dec. 2013.

[3] X. Fu and H. Minn, "Initial uplink synchronization and power control (ranging process) for OFDMA systems," in *Proc. IEEE Global Commun. Conf.*, Dec. 2004, vol. 6, pp. 3999–4003.

[4] Y. Zhou, Z. Zhangm, and X. Zhou, "OFDMA initial ranging for IEEE 802.16e based on time-domain and frequency-domain approaches," in *Proc. Int. Conf. Commun. Technol.*, Nov. 2006, pp. 1–5.

[5] Y. Lin, S. Su, and H. Wang, "A low complexity method of initial ranging for IEEE 802.16e OFDMA systems," in *Conf. Adv. Commun. Technol.*, Feb. 2009, vol. 2, pp. 1137–1141.

[6] H. A. Mahmoud, H. Arslan, and M. K. Ozdemirb, "An efficient initial ranging algorithm for WiMAX (802.16e) OFDMA," *Comput. Commun.*, vol. 32, no. 1, pp. 159–168, Jan. 2009.

[7] X. Fu, Y. Li, and H. Minn, "A new ranging method for OFDMA systems," *IEEE Trans. Wireless Commun.*, vol. 6, no. 2, pp. 659–669, Feb. 2007.

[8] J. Zeng and H. Minn, "A novel OFDMA ranging method exploiting multiuser diversity," *IEEE Trans. Commun.*, vol. 58, no. 3, pp. 945–955, Mar. 2010.

[9] L. Sanguinetti, M. Morelli, and H. Vincent Poor, "An ESPRIT-based approach for initial ranging in OFDMA systems," *IEEE Trans. Commun.*, vol. 57, no. 11, pp. 3225–3229, Nov. 2009.

[10] L. Sanguinetti, M. Morelli, and H. Vincent Poor, "A robust ranging scheme for OFDMA-based networks," *IEEE Trans. Commun.*, vol. 57, no. 8, pp. 2441–2452, Aug. 2009.

[11] M. Ruan, M. C. Reed, and Z. Shi, "Successive multiuser detection and interference cancelation for contention based OFDMA ranging channel," *IEEE Trans. Wireless Commun.*, vol. 9, no. 2, pp. 481–487, Feb. 2010.

[12] C. L. Lin and S. L. Su, "A robust ranging detection with MAI cancellation for OFDMA systems," in *Conf. Adv. Commun. Technol.*, Feb. 2011, pp. 937–941.

[13] L. Sanguinetti and M. Morelli, "An initial ranging scheme for the IEEE 802.16 OFDMA uplink," *IEEE Trans. Wireless Commun.*, vol. 11, no. 9, pp. 3204–2315, Sep. 2012.

[14] A. P. Dempster, N. M. Laird, and D. B. Rubin, "Maximum likelihood form incomplete data via the EM algorithm," *J. R. Stat. Sco. B*, vol. 39, no. 1, pp. 1–38, 1977.

[15] H. Dogan, "EM or SAGE based ML channel estimation for uplink DS-CDMA systems over time-varying fading channels," *IEEE Commun. Lett.*, vol. 12, no. 10, pp. 740–742, Oct. 2008.

[16] A. Kocian, I. Land, and B. H. Fleury, "Joint channel estimation, partial successive interference cancellation, and data decoding for DS-CDMA based on the SAGE algorithm," *IEEE Trans. Commun.*, vol. 55, no. 6, pp. 1231–1241, Jun. 2007.

[17] A. Kocian and B. H. Fleury, "EM-based joint data detection and channel estimation of DS-CDMA signals," *IEEE Trans. Commun.*, vol. 51, no. 10, pp. 1709–1720, Oct. 2003.

[18] N. Kabaoglu, "SAGE based suboptimal receiver for downlink MC-CDMA systems," *IEEE Commun. Lett.*, vol. 15, no. 12, pp. 1381–1383, Dec. 2011.

[19] M. Guenach, M. Marey, H. Wymeersch, and H. Steendam, "Turbo estimation and equalization for asynchronous uplink MC-CDMA," *IEEE Trans. Wireless Commun.*, vol. 7, no. 4, pp. 1217–1226, Apr. 2008.

[20] F. Bellili, A. Methenni, and S. Affes, "Closed-form CRLBs for SNR estimation from turbo-coded BPSK-, MSK-, square-QAM-modulated signals," *IEEE Trans. Signal Process.*, vol. 62, no. 15, pp. 4018–4033, Aug. 2014.

Qiwei Wang was born in Henan, China, in 1987. He received the B.S. degree in communication engineering from Harbin University of Science and Technology, Harbin, China, in 2009 and the M.S. degree in communication and information systems from Xidian University, Xi'an, China, in 2012. He is currently working toward the Ph.D. degree in communication and information systems with Xidian University.

His current research interests focus on uplink synchronization in OFDMA systems, including the initial ranging process in WiMAX systems, the random access procedure in LTE systems, multi-user detection and parameters estimation, and coordinated multipoint, etc.

Guangliang Ren (M'06) was born in Jiangsu, China, in 1971. He received the B.S. degree in communication engineering from Xidian University, Xi'an, China, in 1993, the M.S. degree in signal processing from the Academy of China Ordnance, Beijing, China, in 1996, and the Ph.D. degree in communication and information systems from Xidian University, in 2006.

He is currently a Professor with the School of Telecommunications Engineering, Xidian University. He is the author of more than 40 research papers in journals and conference proceedings, such as IEEE Transactions on Communications, IEEE Transactions on Vehicular Technology and an author or coauthor of three books. His research interests include wireless communication and digital signal processing, particularly multiple-input-multiple-output systems, WiMax, LTE, etc.